Lab on a Chip

Miniaturisation for chemistry, physics, biology, & bioengineering
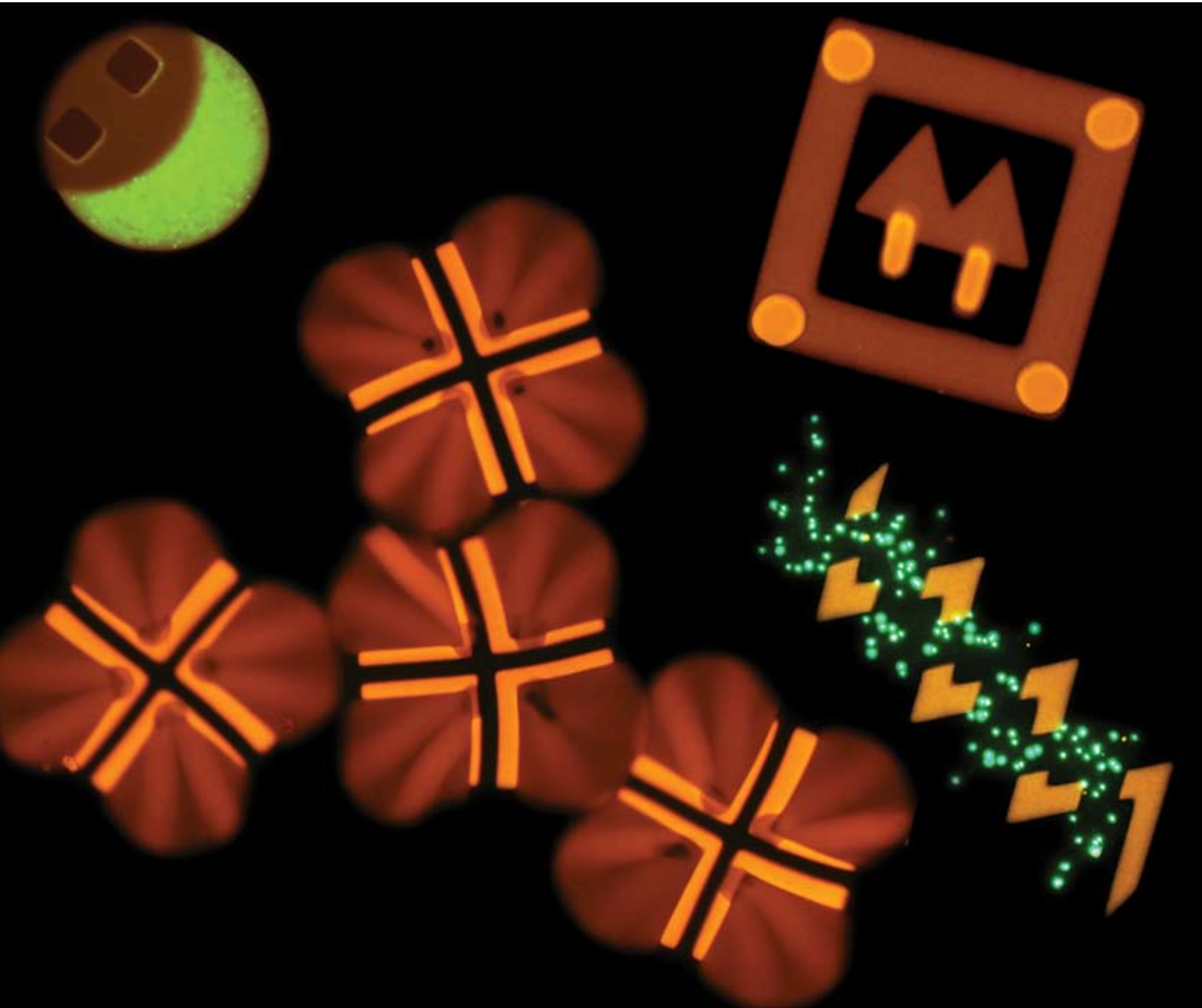
Lock release lithography for 3D and composite microparticles†

Ki Wan Bong, Daniel C. Pregibon and Patrick S. Doyle*

We present a method called "Lock Release Lithography (LRL)" that utilizes a combination of channel topography, mask design, and pressure-induced channel deformation to form and release particles in a cycled fashion. This technique provides a means for the high-throughput production of particles with complex 3D morphologies and composite particles with spatially configurable chemistries. In this work, we demonstrate a diverse set of functional particles including those displaying heterogeneous swelling characteristics and containing functional entities such as nucleic acids, proteins and beads.

Particles with three-dimensional (3D) morphologies and configurable chemistries hold great potential for a host of applications in drug delivery,[1] tissue engineering,[2–4] optics[5] and electromechanics.[6] Of particular interest, patterned particles with precisely positioned chemistries could provide the building blocks for self-assembled, dynamic structures with complex functionality.[7] Self-assembled 3D electronic circuits would give one implication of those applications.[8] Despite their enormous potential, 3D and composite particles cannot be efficiently synthesized on a large scale using current methodologies.[9–13]

Multiphoton fabrication[9] is a well-known method for synthesizing 3D structures as the technique provides unparalleled control of morphology in all dimensions. In spite of the advantage, this direct drawing technique is prohibitively time-consuming. For higher throughput, 3D particles can be generated using a layer-by-layer process with photo resists.[10,11] Unfortunately, these materials are not ideal for many applications and the chemical patterning is limited to layered motifs. Three-dimensional particles can alternatively be generated using the PRINT method,[12] where particles are shaped using a 3D mold. While Janus PRINT particles can be made by sequentially filling the mold with different materials, this approach will only yield simple "striped" material patterns on a particle and, to the best of our knowledge, particles with more than two stripes have not been synthesized.[13]

Here, we introduce lock release lithography (LRL), built off of continuous-flow[14] and stop-flow lithography (SFL).[15] LRL significantly extends the capabilities of SFL to allow for the production of 3D particles which contain intricately patterned chemical regions, well beyond a striped motif.

Department of Chemical Engineering, Massachusetts Institute of Technology, 77 Massachusetts Avenue, Cambridge, MA, 02139, USA. E-mail: pdoyle@mit.edu; Fax: +1 617 258 5042; Tel: +1 617 253 4534
† Electronic supplementary information (ESI) available: Details of the materials, the microfluidic device, the stop-flow lithography setup, and the photopolymerization setup are given as supplementary information. See DOI: 10.1039/b821930c

LRL uses a combination of channel topography, mask features, and pressure-induced channel deformation. The process consists of (1) stopping the flow of a UV-sensitive monomer stream through a microfluidic channel, (2) lithographically printing structures that are "locked" into regions with multi-level channel topography, and (3) inducing channel deformation *via* high pressure to release structures for harvesting.

In the example shown in Fig. 1, we use a channel with positive relief features in the topography (*i.e.* post structures protruding from the channel ceiling) to lock in an array of particles that are formed by 75 ms of UV exposure through a transparency mask using a standard fluorescence microscope. Particle morphology is defined
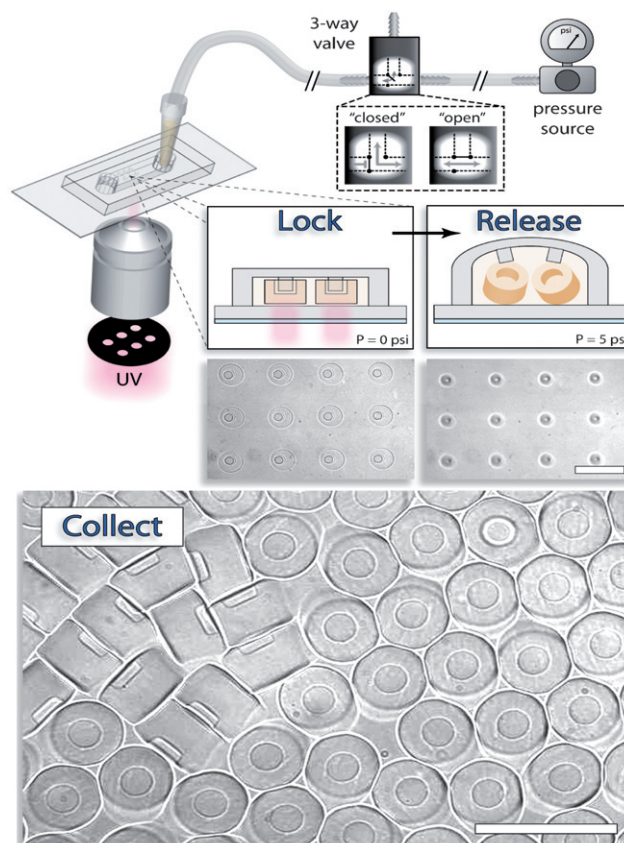

Fig. 1 Process of lock release lithography. First, structures are polymerized by shining bursts of UV light through a transparency mask and a microscope objective. The particles with shapes determined by the mask and channel topography, are "locked" by relief structures in the channel topographies. Particles are "released" with channel deflection after a relatively high pressure (~ 5 psi) is applied to initiate flow. Shown is a differential interference contrast (DIC) image of a collection of 3D particles with micro-cavity in the channel reservoir. Scale bars are 100 μm.

by a combination of mask feature shape and channel topography. Locked into the three-dimensional relief, particles remain immobilized until a relatively high pressure (~5 psi) is applied to the poly-(dimethylsiloxane) (PDMS) channel to initiate flow and deflect the channel beyond the point of particle release. Using an automated valving system shown in the right top of Fig. 1, the flow is then stopped *via* pressure release, and the process is repeated, thus allowing the formation of 3D particles in an automated, semi-continuous manner. For more details about the automated system, see ref. 15. The ratio of monomer which is converted into particles to that which is used to flush out the channel between polymerization cycles is approximately 1 : 50.

With the need for periodic channel deformation, this process is well-suited by stop-flow lithography, but incompatible with continuous-flow techniques.[14,16] Recently, continuous-flow lithography was used to fabricate finned structures in "railed" channels for guided self-assembly.[16] However, without release, this process cannot be used to generate diverse topographies. For example, the cup-shaped particles in Fig. 1 cannot be released without channel deflection. Several other advantages are afforded by stop-flow, including improved resolution and a higher throughput up to $10^6 \sim 10^7$ particles per hour using a single microscope.[15]

The key to LRL is obtaining sufficient channel deformation to release polymerized structures. For thin PDMS channels, the deformation is determined by classical elasticity theory[17] as $\Delta h_{max} \approx 0.142PW^4/Et^3$ where P is the pressure, W is the width of the channel, E is the young's modulus of PDMS, and t is channel thickness. In agreement with theory, we observed that particles with 20 µm tall locking structures were released at 5 psi in a 500 µm wide channel, which had a ceiling PDMS thickness around 200 µm. For 1 mm wide channels, the equation reveals that 5 psi pressure could provide enough deflection to release 3D particles with relief features of ~ 250 µm. To exploit maximum channel deformation and ensure safe particle release, particles are polymerized near the channel inlet, channels are kept fairly wide, and the channel region near the outlet designed to be taller than the particles.

Because LRL is a variant of flow lithography,[14–16] the oxygen lubrication layer near channel surfaces is expected to be a ~ 1 µm thick.[14] Thus, the achieved particle size in LRL is limited to micrometer ranges. Particle and feature size resolutions are dictated by the optical resolution and the ability to replicate features from the channel wall/ceilings. The typical optical resolution we achieve with our setup is ~1 µm. Replicating 3D features on a wall is limited by the oxygen inhibition layer which is also ~1 µm in the current experiments. Smaller inhibition layers, and hence smaller replicated features, can be achieved by controlling the ambient oxygen concentration. Topographical channel features used in LRL are at least a few microns in size, larger than the UV wavelength (~360 nm), such that optical interference can be disregarded.

For synthesis, we typically use monomers based on poly(ethylene glycol), as this material is bio-friendly, highly tunable, and can be functionalized with a variety of biomolecules.[18,19] As shown in Fig. 2, we synthesized a variety of 3D particles with unique mask shapes and channel topographies. We used negative dot pattern topographies with square mask features to generate 3D particles with pillars (Fig. 2a,b). Positive relief topographies can be used to generate dishes and cups – particles with voids that could potentially be filled with active components or cells (Fig. 2h). Importantly, LRL can be performed with the same channel and varying masks to give a variety of
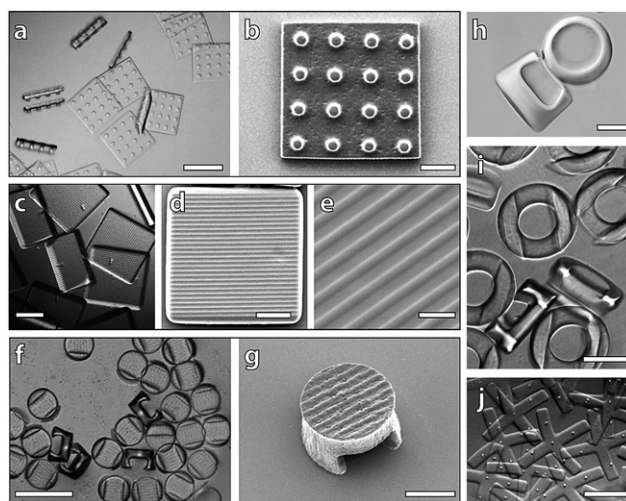

Fig. 2 DIC and scanning electron microscope (SEM) images of 3D particles. (a),(b) Squares with 10 µm high pillars using a 20 µm high channel with negative dot patterns on its ceiling and a square mask. (c)–(e) Squares with 1 µm high line-space patterns using a 30 µm high channel with negative line-space patterns on its floor and a square mask. (f),(g) Table-like 3D particles with 1 µm high line-space patterns on the top and 30 µm high supports on the bottom using a 30 µm high channel with negative line-space patterns on both sides and a circle mask. (h) Micro-cups with 30 µm deep voids using a 60 µm high channel with positive dot patterns on its ceiling and a circle mask. (i),(j) Variants using 30 µm high channels with same kinds of topographies of negative line-space and dots on their ceiling, but different ring and cross masks. Scale bars are 200 µm (a,f,j), 100 µm (c,i), 50 µm (b,d,g,h), and 10 µm (e).

particle morphologies (Fig. 2i,j). As shown in Fig. 2c and 2d, we could use very fine 3.5 µm line-space patterns (with 7 µm pitch) to produce particles with precisely defined linear features. These troughs could be oriented with the particle edges (Fig. 2c,d) or made to be oblique by simply rotating the mask with respect to the channel.

To demonstrate that both channel floor and ceiling topographies could be used to dictate morphology, we synthesized table-like structures with large relief features on one side and a highly resolved 5 µm line-space pattern on the other (Fig. 2f,g). These particles demonstrate the ability to combine coarse and fine features into particle topography. Morphologies generated with LRL can be more complicated depending on the mold used to generate the channel topographies, and the mask used to polymerize the particles. Molds generated using standard lithography can be multi-tiered, rounded, or slanted,[20] while virtually any topography can be achieved using multiphoton fabrication.[9] The transparency masks used to generate particles can have virtually any two-dimensional shape, can be grayscale[21,22] to provide variability in height along particles, and can be used in conjugation with interference masks to give finely tuned microporous structures.[23] However, in its current inception, LRL is not suitable for the preparation of interlocking (like chain links) features or particles with internal hollow structures.

The most attractive feature of LRL is that the release time is controllable. Because particle release occurs at a critical pressure (related to deformation), lower pressures can be used to exchange the monomer without unlocking the particles – this allows the subsequent addition of new chemistries. As such, LRL can be used
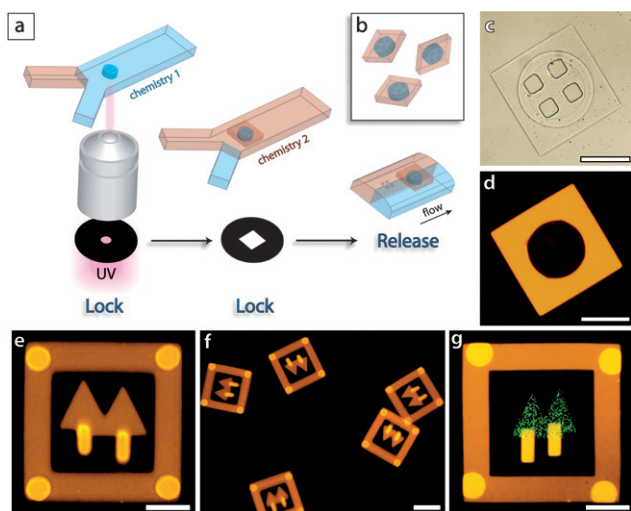
Fig. 3 Synthesis of composite particles. (a),(b) A schematic diagram showing the synthesis of composite particles. Locked structures with chemistry 1 are covalently linked to chemistry 2 through mask overlap and UV exposure after fluidic exchange with low pressure. Then, the composite structures are released by high pressure in both flows. (c),(d) DIC and fluorescence microscopy images of the particle shown in (a),(b). Two streams containing PEG-DA and PEG-DA with rhodamine-labeled monomer were used to respectively present chemistry 1 and chemistry 2. (e),(f) Fluorescence microscopy images of composite particles with "autumn trees" in a frame. The six locks appear brighter than the rest of the fluorescent region since they are thicker. (g) Fluorescence microscopy image of composite particles with "spring trees" in a frame. Scale bars are 100 μm (c,d,f) and 50 μm (e,g).

efficiently to generate composite particles with multiple precisely positioned chemistries. The process is shown schematically in Fig. 3a. First, the multi-inlet channel is filled with chemistry #1 and locked 3D structures are polymerized. Then, by adjusting the pressures of the inlet streams (but keeping them below ∼ 1 psi), a second chemistry replaces the first without displacing the locked particle structure. A unique mask can be used with this chemistry to polymerize distinct particle features that are covalently linked to the locked particles *via* overlap. Finally, a high pressure flow (∼ 10 psi) is used to release the composite particles (Fig. 3b).

To demonstrate the synthesis of composite particles, we used two chemistries, both with poly(ethylene glycol) diacrylate (PEG-DA) monomer and one with a fluorescent monomer (rhodamine-acrylate, orange) to easily distinguish the chemistries *via* fluorescence after polymerization. We used positive-relief locks to synthesize patterned particles with a circular center and square exterior (Fig. 3c,d), and negative-relief locks to make more intricate particles with interior features and borders (Fig. 3e,f). Both particle types were generated using two polymerization steps. This approach can be applied to any number of unique chemistries. Shown in Fig 3g is one example that applies three chemistries. The particles were synthesized by the same process using one more PEG-DA monomer stream with 500 nm fluorescent beads. In this case, the sequence of polymerization is PEG-DA with fluorescent rhodamine-acrylate, then PEG-DA with fluorescent beads, and lastly PEG-DA with no fluorescent entities. Due to lag times associated with fluidic exchange and mask alignment, the throughput for composite particles depends on how many chemistries are applied. As the number of different chemistries

incorporated into a particle increases, the throughput decreases. When two chemistries are used, we can generate ∼ 10³ composite particles with dimensions of 50 μm per hour on our current system. This can be expedited in the future using dynamic mask systems.[24]

The overlap regions of multifunctional particles can be designed to provide interwoven chemistries or excluded chemistries, depending on the pore size of the initial material and the size of entities included in subsequent monomers. When the pore size is large enough for molecules to leech in, the result is an interwoven blend of the two chemistries. However, when entities included in the monomer blend are larger than the pore size of the existing structure, those entities are excluded from the overlap region, resulting in a segregation of chemistries. Examples of interwoven and excluded chemistries are shown in Fig. 4a. We prepared "Venn diagram-like" particles to
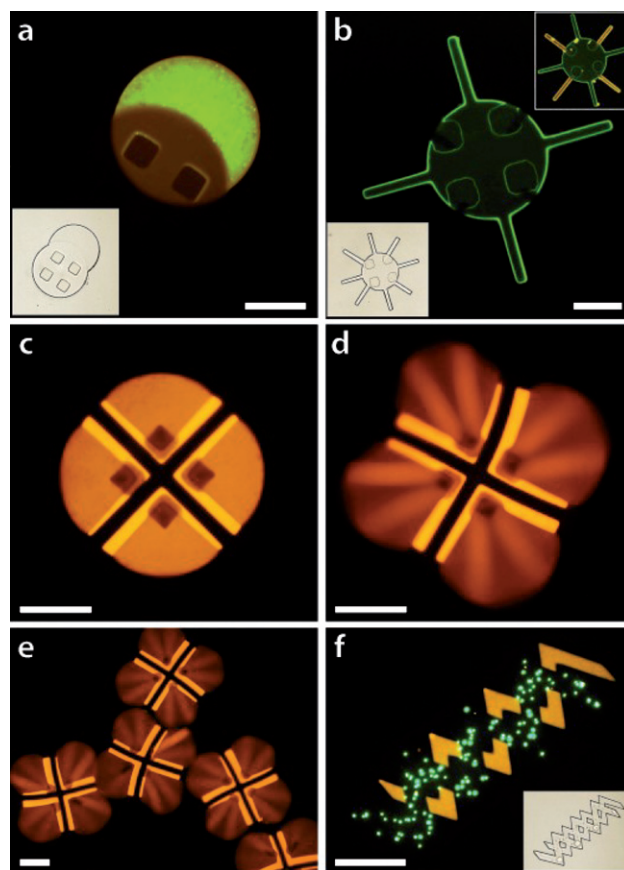

Fig. 4 Functional particles. (a) Fluorescence and DIC (insert, outlined for clarity) images of "Venn diagram" particle demonstrating interwoven (fluorescent monomer, orange) and excluded chemistries (beads, green) in polymerization overlap region. (b) Fluorescence and DIC (insert, outlined for clarity) images of a DNA detector particle with distinct probe regions. Shown are fluorescent images of a particle after incubation with target #1 (green) or both targets #1 (green, insert in the top right corner) and #2 (red, insert in the top right corner). (c)–(e) Fluorescence images of particles with pH-responsive fins and a cross-shaped rigid support. The particle keeps its original 2D circle shape in low pH (c), while in an alkaline pH, the fins bloom to form a 3D flower-like structure (d). (f) Fluorescence and DIC (insert, outlined for clarity) images of overlapping zig-zag-shaped particles with encapsulated entities. One strand contains 2 μm green fluorescent beads while the other has 5 nm red fluorescent streptavidin protein. In all DIC images, particles have been outlined for clarity. Scale bars are 50 μm (a,b), and 100 μm (c–f).

investigate the incorporation of chemistries in the overlap regions. The first chemistry was a pure PEG hydrogel with a pore size expected to be ~ 1 nm.[25] The second chemistry was PEG with the addition of rhodamine-acrylate and 50 nm green fluorescent beads. As can be seen, the fluorescent monomer penetrated the initial gel structure and was incorporated in the overlap region while the colloidal entities were excluded.

We exploited the ability to spatially arrange multiple chemistries in LRL to prepare particles with diverse functionalities. Fig. 4b shows a DNA detector particle[18] with distinct probe regions. The interior region and four wings contained DNA probe #1, while the other four wings contained probe #2. The particles were incubated with target #1 (which was labeled with green fluorescence, FITC) or both targets (target #2 was labeled with red fluorescence, Cy3) at 10 nM at 37 °C for 30 min. Fluorescence images confirm that the target oligomers hybridize only with their complementary probe regions. We also generated particles with opposing chemistries – specifically swelling and non-swelling. Swelling chemistries were achieved using PEG/acrylic acid monomer blends, which are well-known to be responsive to changes in pH. We made particles with a cross-shaped support and pH-responsive, fluorescent fins between each arm (Fig. 4c–e). In acidic conditions (pH ~ 3), these particles keep their original 2D body (Fig. 4c), while in neutral to alkaline conditions (pH ~ 8), the responsive fins bloom to form a 3D flower-like structure (Fig. 4d,e). Lastly, we demonstrate the generation of particles with various encapsulated entities that are organized in complex hierarchies. We made particles with overlapping zig-zag-shaped chemistries, one of which was laden with 2 μm fluorescent beads (FITC, green), and the other with 5 nm fluorescent protein (streptavidin-phycorytherin, red) (Fig. 4f). This process can be used to encapsulate living cells, stimuli, or nutrients with precise control over position, which has implications for applications in tissue engineering. Compared to other hydrogel particle-based approaches to engineering tissue constructs,[2] we can prepare more precise and intricate building blocks in a scalable and highly homogeneous manner.

In conclusion, we have demonstrated that LRL can be used to easily generate a diverse range of 3D and multifunctional composite particles through the association of channel topography, mask features, and pressure-induced channel deformation. The computer-automated method provides high resolution and high-throughput, similar to that seen in standard stop-flow lithography.[15] Also, locked structures can be built upon to generate complex, composite particles with a broad range of potential chemistries, interwoven or excluded, with incorporated entities including nucleic acids, proteins, or cells. For example, the length scales in LRL are ideally suited to generating tissue engineering mesoconstructs each containing multiple cell lines which are precisely positioned within the particle.[2,19] In addition, the juxtaposition of swelling and stiff materials can be exploited to create particles that can undergo dramatic shape changes. Degradable polymers can be used to create microparticles which controllably evolve or fragment over time. We envision that this technology will provide a simple but powerful means to mass-produce functional units for microfluidic operations, filtration systems, and tissue engineering constructs.

Notes and references

1 D. A. LaVan, T. McGuire and R. Langer, *Nat. Biotechnol.*, 2003, **21**, 1184–1191.
2 Y. Du, E. Lo, S. Ali and A. Khademhosseini, *Proc. Natl. Acad. Sci. USA*, 2008, **105**, 9522–9527.
3 N. A. Peppas, J. Z. Hilt, A. Khademhosseini and R. Langer, *Adv. Mater.*, 2006, **18**, 1345–1360.
4 W. G. Koh, L. J. Itle and M. V. Pishko, *Anal. Chem.*, 2003, **75**, 5783–5789.
5 P. Vukusic and J. R. Sambles, *Nature*, 2003, **424**, 852–855.
6 C. M. Waits, B. Morgan, M. Kastantin and R. Ghodssi, *Sensors and Actuators A*, 2005, **119**, 245–253.
7 S. C. Glotzer and M. J. Solomon, *Nat. Mater.*, 2007, **6**, 557–562.
8 D. H. Gracias, J. Tien, T. L. Breen, C. Hsu and G. M. Whitesides, *Science*, 2000, **289**, 1170–1172.
9 C. N. LaFratta, J. T. Fourkas, T. Baldacchini and R. A. Farrer, *Angew. Chem. Int. Ed.*, 2007, **46**, 6238–6258.
10 S. L. Tao, K. Popat and T. A. Desai, *Nat. Protocols*, 2006, **1**, 3153–3158.
11 C. J. Hernandez and T. G. Mason, *J. Phys. Chem. C*, 2007, **111**, 4477–4480.
12 J. P. Rolland, B. W. Maynor, L. E. Euliss, A. E. Exner, G. M. Denison and J. M. DeSimone, *J. Am. Chem. Soc.*, 2005, **127**, 10096–10100.
13 S. E. A. Gratton, S. S. Williams, M. E. Napier, P. D. Pohlhaus, Z. Zhou, K. B. Wiles, B. W. Maynor, C. Shen, T. Olafsen, E. T. Samulski and J. M. Desimone, *Acc. Chem. Res.*, 2008, DOI: 10.1021/ar8000348.
14 D. Dendukuri, D. C. Pregibon, J. Collins, T. A. Hatton and P. S. Doyle, *Nat. Mater.*, 2006, **5**, 365–369.
15 D. Dendukuri, S. S. Gu, D. C. Pregibon, T. A. Hatton and P. S. Doyle, *Lab Chip*, 2007, **7**, 818–828.
16 S. E. Chung, W. Park, S. Shin, S. A. Lee and S. Kwon, *Nat. Mater.*, 2008, **7**, 581–587.
17 W. C. Young, in *Roark's Formulas for Stress and Strain* (Eds: H. B. Crawford, S. Thomas), McGraw-Hill, New York, 1989, 457.
18 D. C. Pregibon, M. Toner and P. S. Doyle, *Science*, 2007, **315**, 1393–1396.
19 P. Panda, S. Ali, E. Lo, B. G. Chung, T. A. Hatton, A. Khademhosseini and P. S. Doyle, *Lab Chip*, 2008, **8**, 1056–1061.
20 M. A. Unger, H. P. Chou, T. Thorsen, A. Scherer and S. R. Quake, *Science*, 2000, **288**, 113–116.
21 J. Atencia, S. Barnes, J. Douglas, M. Meacham and L. E. Locascio, *Lab Chip*, 2007, **7**, 1567–1573.
22 D. Dendukuri, P. Panda, R. Haghgooie, J. M. Kim, T. A. Hatton and P. S. Doyle, *Macromolecules*, 2008, **41**, 8547–8556.
23 J. H. Jang, D. Dendukuri, T. A. Hatton, E. L. Thomas and P. S. Doyle, *Angew. Chem. Int. Ed.*, 2007, **46**, 9027–9031.
24 S. E. Chung, W. Park, H. Park, K. Yu, N. Park and S. Kwon, *Appl. Phys. Lett.*, 2007, **91**, 041106.
25 M. B. Mellott, K. Searcy and M. V. Pishko, *Biomaterials*, 2001, **22**, 929–941.